Supplementary Information for "Common physical framework explains phase behavior and dynamics of atomic, molecular and polymeric network-formers"

Stephen Whitelam[1],* Isaac Tamblyn[2],† Thomas K. Haxton[1], Maria B. Wieland[3], Neil R. Champness[4], Juan P. Garrahan[3], and Peter H. Beton[3‡]
[1] *Molecular Foundry, Lawrence Berkeley National Laboratory, 1 Cyclotron Road, Berkeley, CA 94720, USA*
[2] *Faculty of Science, University of Ontario Institute of Technology, Oshawa, Ontario L1H 7K4, Canada*
[3] *School of Physics and Astronomy, University of Nottingham, Nottingham NG7 2RD, UK*

S1. SUMMARY OF SUPPLEMENT

Section S2 describes our procedure for processing experimental images.

Fig. S1 and Fig. S2 supplement Fig. 2 of the main text. Fig. S3 supplements Figs. 3–5 of the main text. Fig. S4 supplements Fig. 3 of the main text. Figs. S5–S9 supplement Figs. 4 and 5 of the main text.

S2. EXPERIMENTAL IMAGE PROCESSING

Image processing: Fig. S1 shows the sequence of image processing steps which were used to convert experimentally acquired STM images into form where polygons can be colourised. The original STM image was first flattened (the gradient is subtracted for each horizontal scanline) using the open source software package WSxM [1] to enhance the overall contrast as shown in Panel A. The image was subsequently converted into a black and white image using the Photoshop CS5 Stamp filter (Photoshop CS5 Extended Version 12.1 x32). This is an extreme contrast function which converts all bright regions above a certain threshold (the covalent network and some defects) to zero intensity black areas, and below threshold dark regions (cavities) to full intensity white areas. The result is in shown in Panel B.

The image was subsequently imported into ImageJ 1.47g (ImageJ 1.47g: Rasband, W.S., ImageJ, U. S. National Institutes of Health, Bethesda, Maryland, USA, `http://imagej.nih.gov/ij/` (1997-2012)) as an 8-bit binary image. This program allows the conversion of the dark lines with finite thickness in Panel B into lines with the width of a single pixel using the Skeletonize tool [2] as shown in Panel C. The network is now a simplified and compact representation of the original network that preserves its key features such as junctions and connectivity.

With the ImageJ 'Analyze Skeleton' plugin all voxels in the skeleton image were tagged and colored depending on their eight neighbors: blue voxels represent end points (less than two neighbors), orange voxels represent slab voxels (exactly two neighbors), and purple voxels represent junction voxels (more than two neighbors). The purple voxel clusters were isolated by applying a color threshold resulting in Panel D. These voxel clusters represent the location of the centers of the molecules in the network.

A path connecting these junctions via straight lines was manually created in Photoshop CS5 to recreate the original network see Panel E. The resulting was checked by overlaying the network over the original image. Missing connections were appended and defective regions omitted. Finally the polygonal cavities were colored manually according to the scheme shown in Fig. 1, main text. Grey areas indicate filled, open, imperfect, or non-determinable cavities as shown

*Electronic address: `swhitelam@lbl.gov`
†Electronic address: `Isaac.Tamblyn@uoit.ca`
‡Electronic address: `Peter.Beton@nottingham.ac.uk`

in Panel F; these may be compared with the original STM image shown in Panel A.

---

[1] I. Horcas, R. Fernandez, J. Gomez-Rodriguez, J. Colchero, J. Gómez-Herrero, and A. Baro, Review of Scientific Instruments **78**, 013705 (2007).

[2] I. Arganda-Carreras, R. Fernández-González, A. Muñoz-Barrutia, and C. Ortiz-De-Solorzano, Microscopy research and technique **73**, 1019 (2010).

[3] L. Lichtenstein, C. Büchner, B. Yang, S. Shaikhutdinov, M. Heyde, M. Sierka, R. Włodarczyk, J. Sauer, and H.-J. Freund, Angewandte Chemie International Edition **51**, 404 (2012).

[4] L. Lichtenstein, M. Heyde, and H.-J. Freund, Physical Review Letters **109**, 106101 (2012).

S3. SUPPLEMENTAL FIGURES

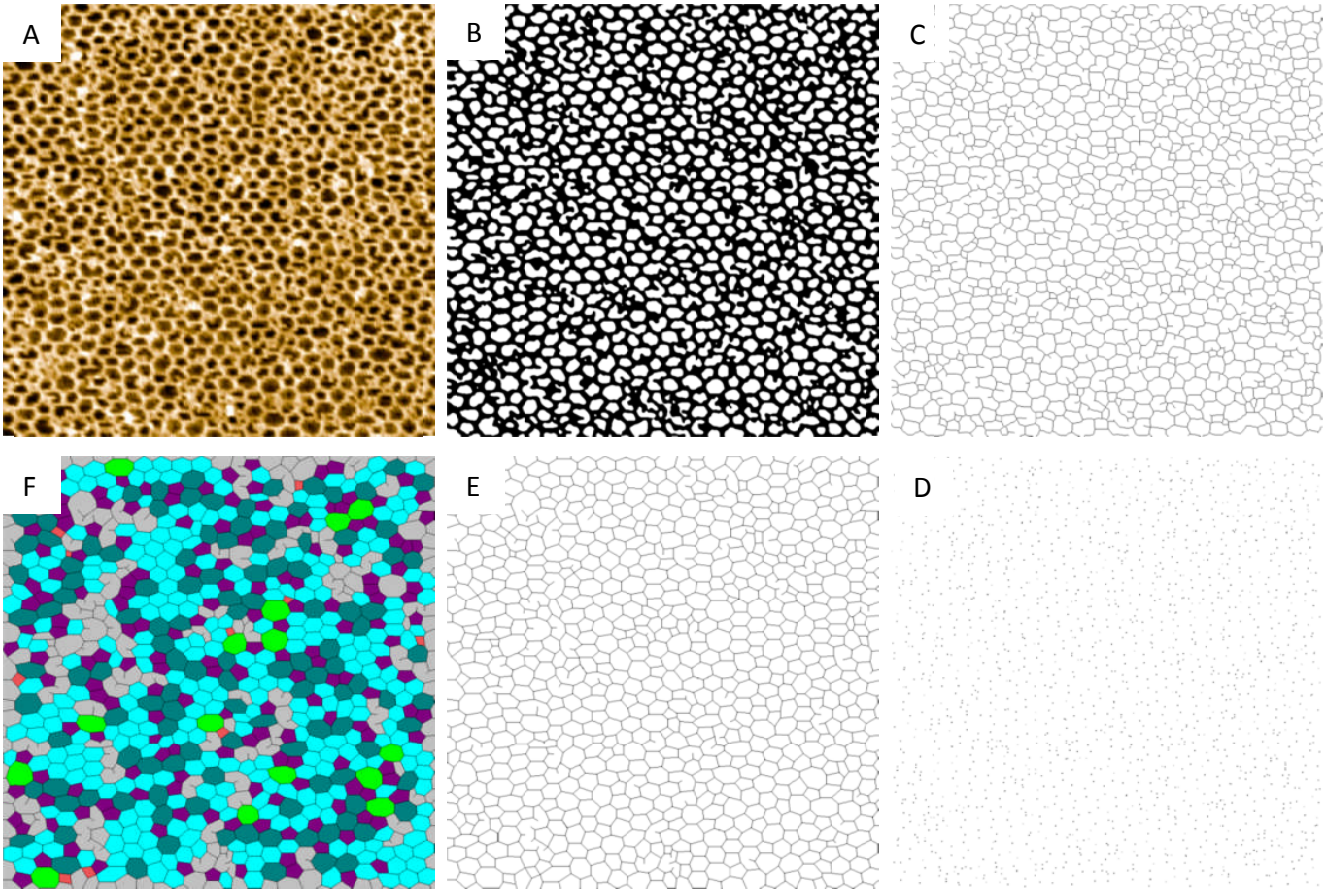

FIG. S1: Supplement to Fig. 2, main text. Processing of STM images to determine polygonal mapping; see Section S2.

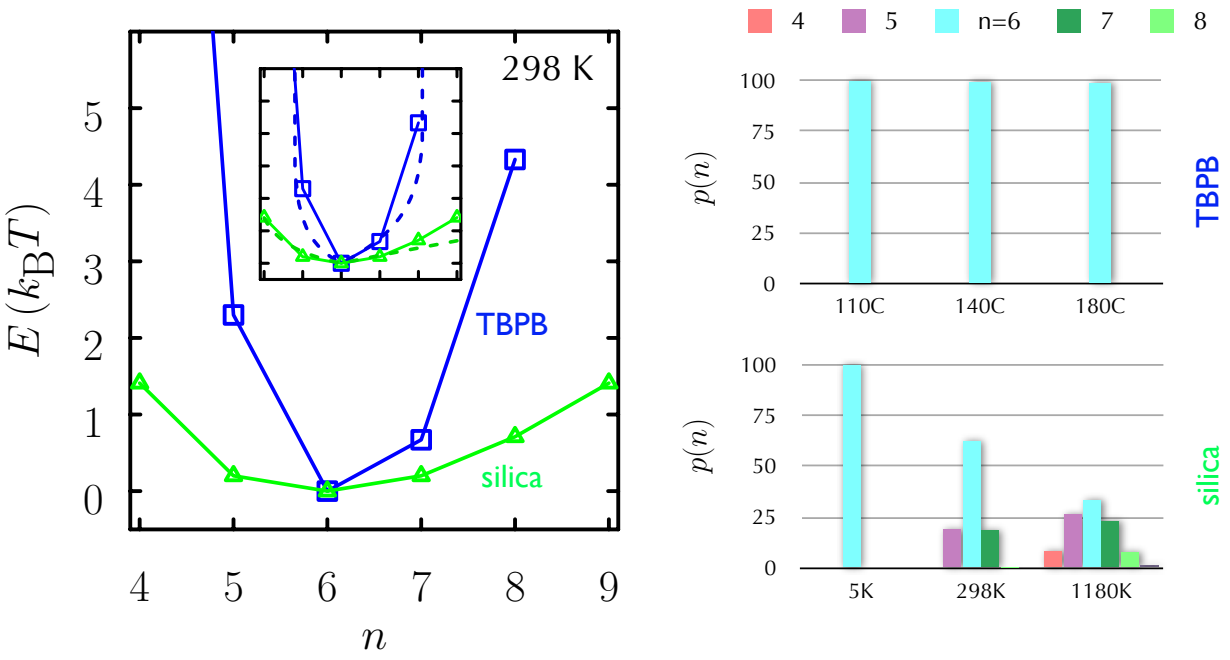

FIG. S2: Supplement to Fig. 2, main text. Energies of isolated regular polygons of TBPB (Fig. 2(b) of main text, reproduced here in blue) and silica (taken from calculations in Ref. [3], shown in green) reveal, using a topological gas estimate (right-hand panel) that only silica was prepared under conditions at which the polygon network was thermodynamically stable: preparation temperatures in [3] exceeded 1000K, while preparation temperatures for the TBPB network did not exceed 180°C. We therefore interpret the behavior shown in panel E of Fig. 1 as thermodynamic phase coexistence between the honeycomb and the polygon network (frozen because of the low temperatures at which images in Refs. [3, 4] were taken). Inset to left panel: comparison of potentials with model collective potential for two different patch widths demonstrate that the model potential's functional form is different to the functional form of the real collective potentials. Despite this difference of detail, the qualitative behavior of both real systems can be captured by the model.

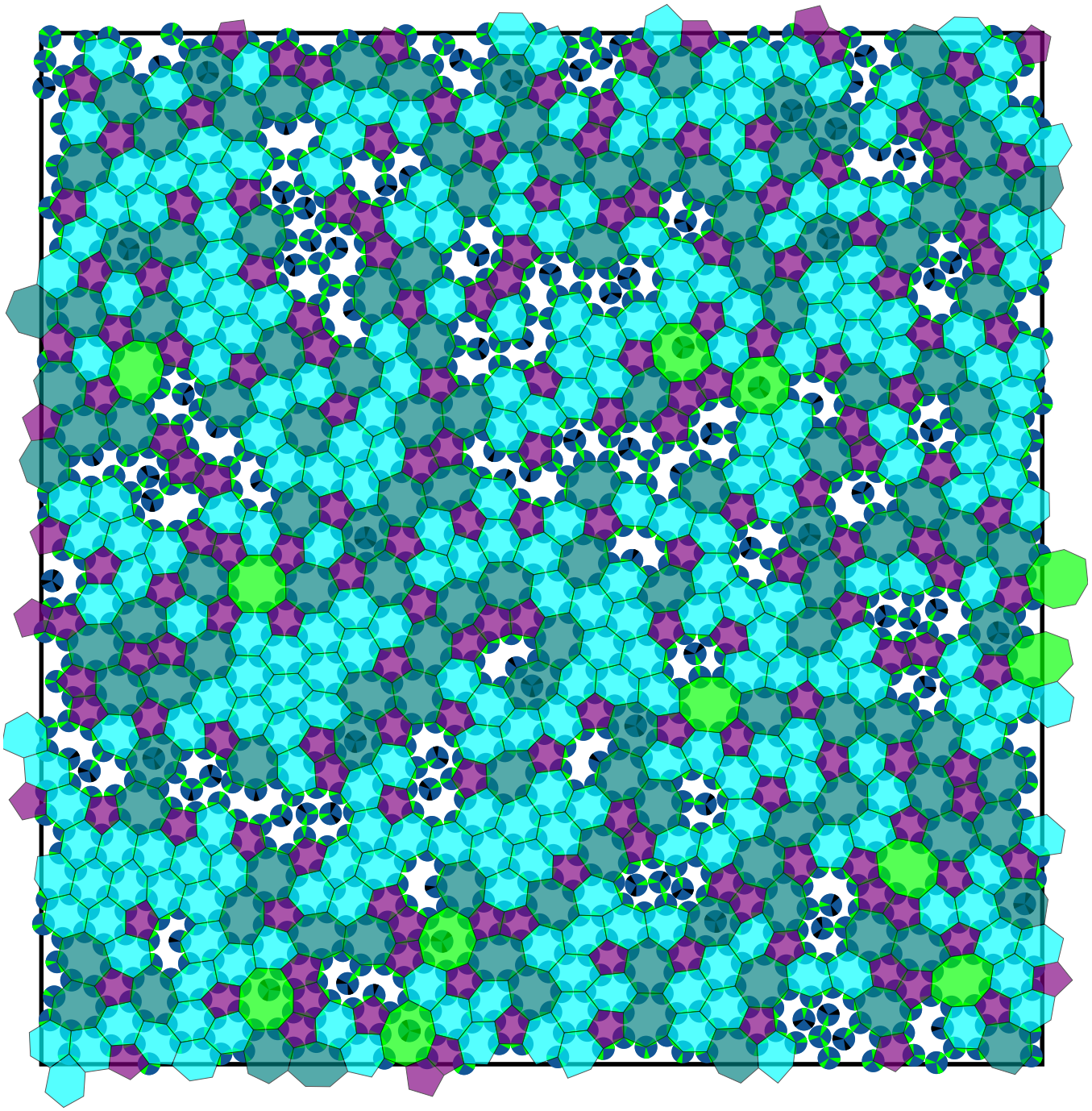

FIG. S3: Supplement to Figs. 3–5, main text. Simulation snapshot showing a hybrid of the disc representation and the polygon representation (simulations are done using discs, and polygons are drawn on top as a guide to the eye). We draw only convex polygons, and draw only polygons that do not enclose other polygons. Note that unbound particles can be caged within polygons.

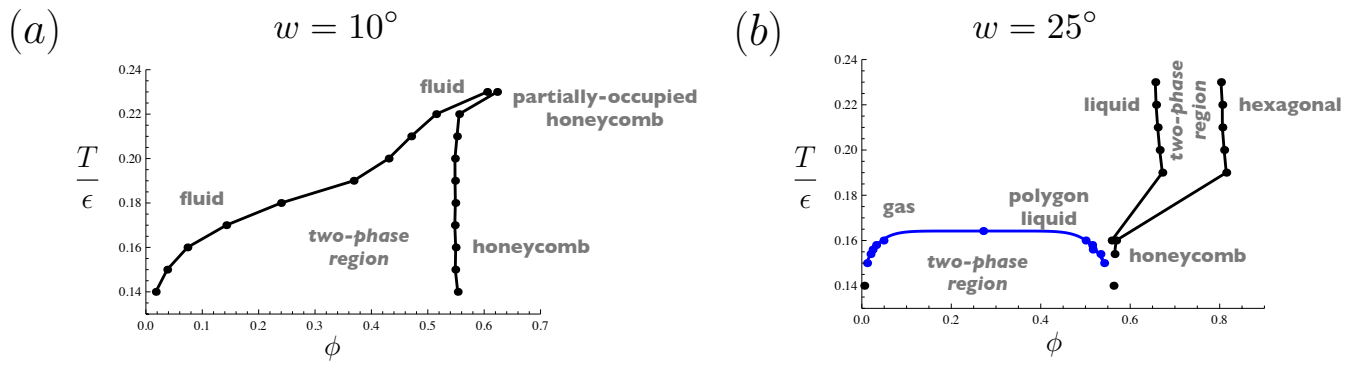

FIG. S4: Supplement to Fig. 3(b), main text. Thermodynamic phase diagrams of the disc model in the temperature-density plane (see Appendix F, main text) show the emergence of a stable gas-polygon liquid binodal, and a regime of stable honeycomb/polygon network coexistence, at large stripe widths. Silica [3] (Fig. 1 panel E) shows what appears to be a similar coexistence.

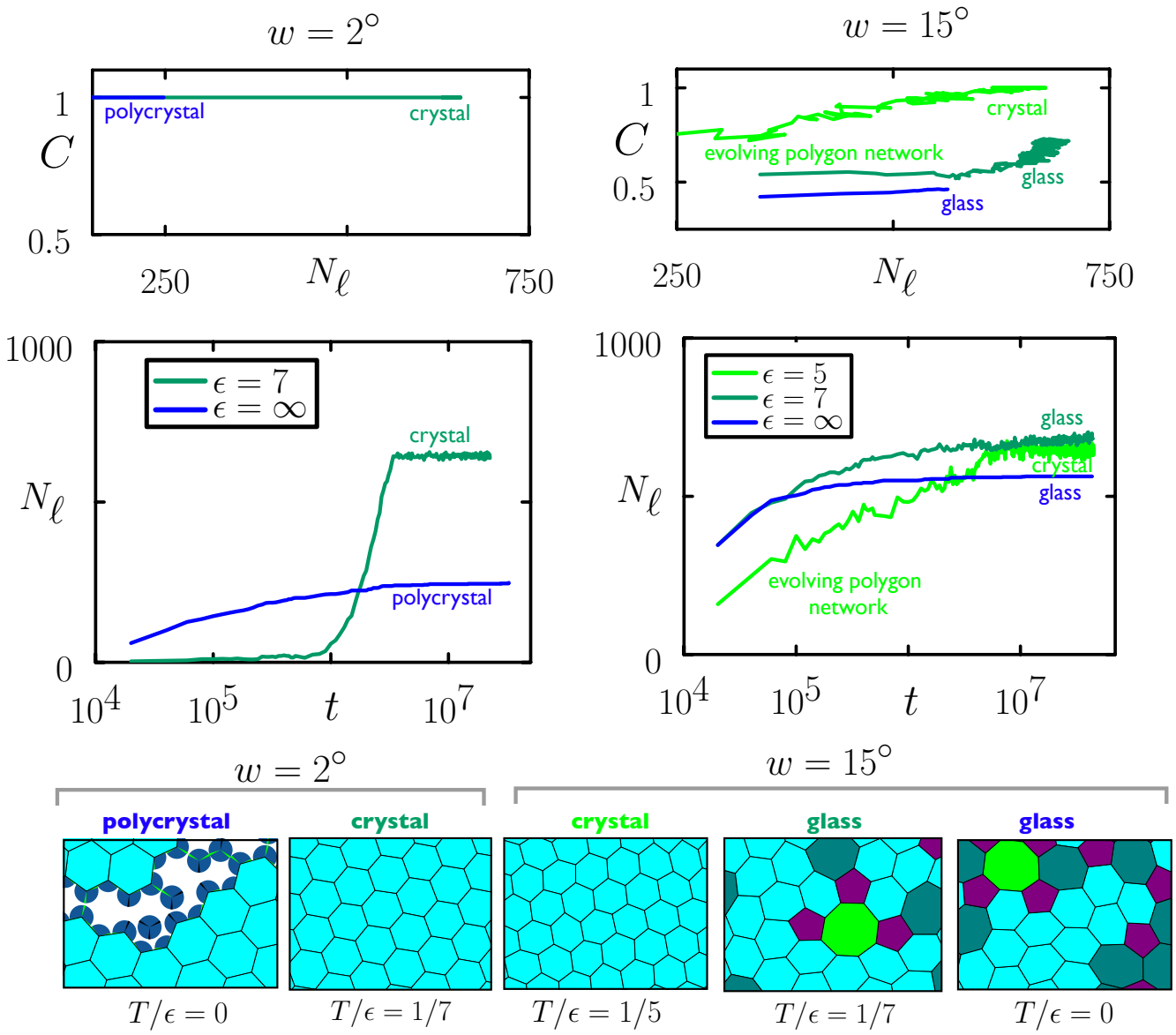

FIG. S5: Supplement to Figs. 4 and 5, main text. C is network crystallinity, the number of hexagons divided by the number of all polygons [4], and N_ℓ is the total number of polygons (loops) in the simulation box. We show the results of dynamical simulations for narrow ($w = 2°$) and moderately wide ($w = 15°$) stripes. Left: When the stripe is narrow, discs self-assemble as polycrystals, regions of hexagonal network separated by grain boundaries. Few grains are formed in the nucleation regime; many grains form in the spinodal regime. Right: When w is larger (still within the regime in which the network is ordered thermodynamically), the first pieces of the self-assembled network are polygons. These coarsen to the honeycomb if bond energies are not too large. Otherwise, networks are trapped, forming glasses.

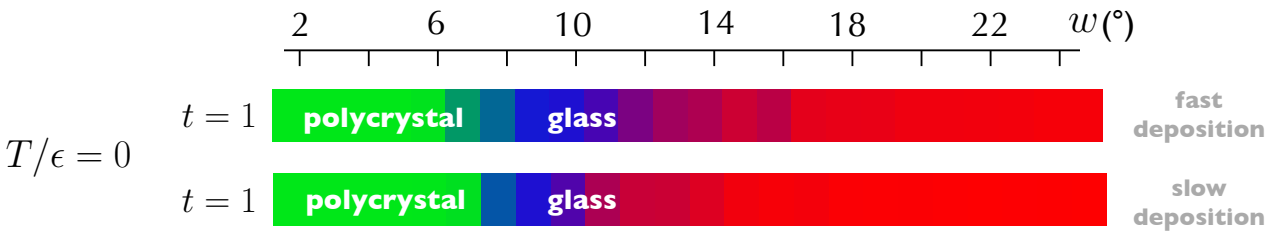

FIG. S6: Supplement to Figs. 4 and 5, main text. Comparison of slow and fast deposition protocols (Appendix G, main text) shows that, given w, structures formed under different dynamical protocols can have different polygon statistics. Nonetheless, the qualitative trends seen are similar.

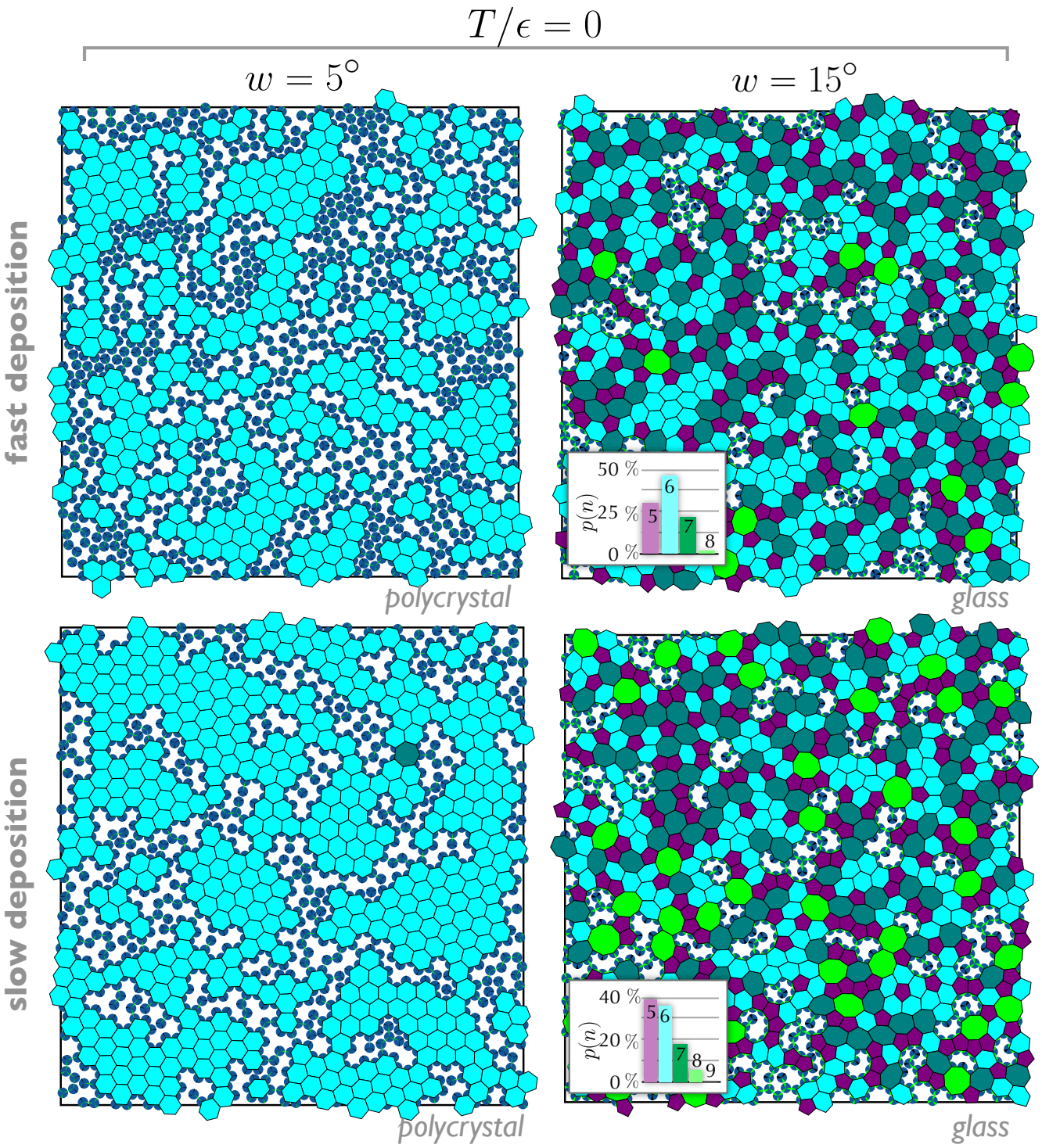

FIG. S7: Supplement to Figs. 4 and 5, main text. Comparison of slow and fast deposition protocols (Appendix G, main text) shows that grain boundary densities within polycrystals, and polygon counts within glasses, are sensitive to details of the dynamical protocols used. The qualitative nature of the structures assembled, however, are not.

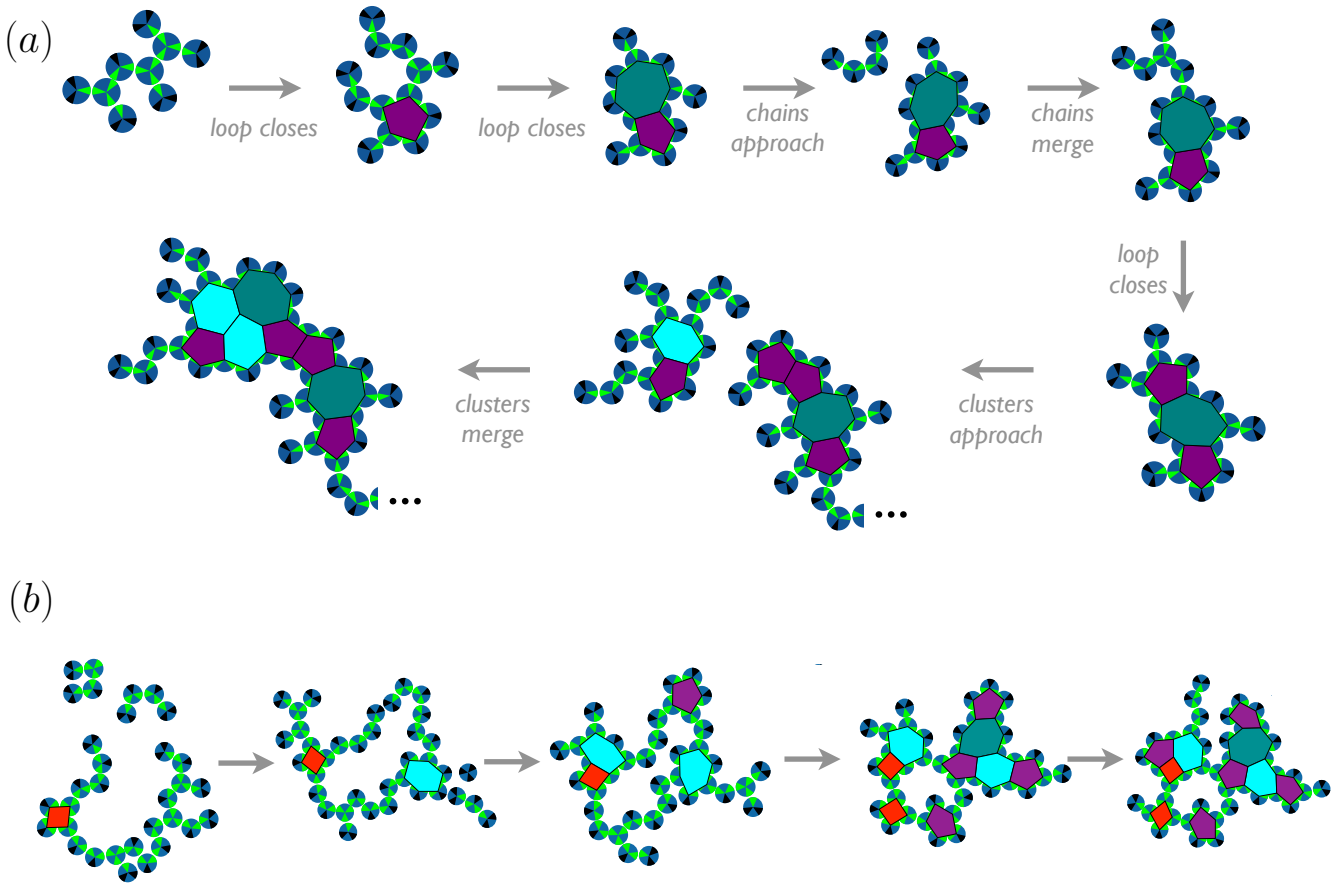

FIG. S8: Supplement to Figs. 4 and 5, main text, demonstrating the collective microscopic motions of discs – such as cluster mergings and loop closings – that generate the polygon statistics at early times for sufficiently large stripe widths: (a) $w = 17°$; (b) $w = 25°$. Subsequent evolution to the honeycomb can occur if disc binding energies are not too strong; otherwise, polygon statistics are 'frozen in', resulting in a glass statistically unrelated to the polygon network thermodynamically stable at large w.

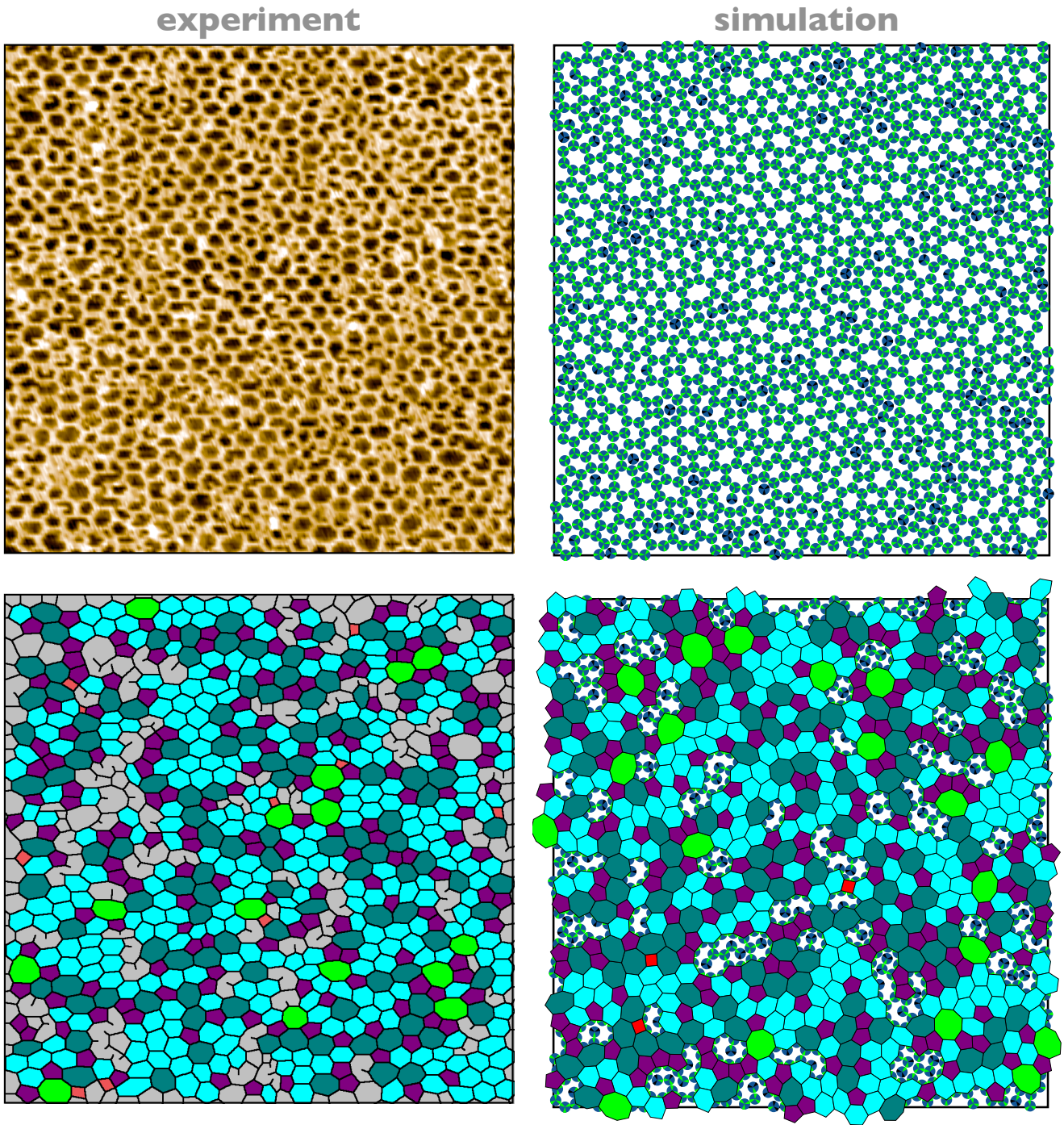

FIG. S9: Supplement to Figs. 4 and 5, main text. There is a strong qualitative similarity between the experimental TBPB network (see Fig. 2(a), main text) and disc networks assembled in the 'glass-forming' regime (here $w = 17°, T/\epsilon = 0$, an enlargement of one of the panels of Fig. 4). Shown top are the particle representations; shown bottom are the polygon representations.